VIEWPOINT

Interpretation of presynaptic phenotypes of synaptic plasticity in terms of a two-step priming process

Erwin Neher[1]

Studies on synaptic proteins involved in neurotransmitter release often aim at distinguishing between their roles in vesicle priming (the docking of synaptic vesicles to the plasma membrane and the assembly of a release machinery) as opposed to the process of vesicle fusion. This has traditionally been done by estimating two parameters, the size of the pool of fusion-competent vesicles (the readily releasable pool, RRP) and the probability that such vesicles are released by an action potential, with the aim of determining how these parameters are affected by molecular perturbations. Here, it is argued that the assumption of a homogeneous RRP may be too simplistic and may blur the distinction between vesicle priming and fusion. Rather, considering priming as a dynamic and reversible multistep process allows alternative interpretations of mutagenesis-induced changes in synaptic transmission and suggests mechanisms for variability in synaptic strength and short-term plasticity among synapses, as well as for interactions between short- and long-term plasticity. In many cases, assigned roles of proteins or causes for observed phenotypes are shifted from fusion- to priming-related when considering multistep priming. Activity-dependent enhancement of priming is an essential element in this alternative view and its variation among synapse types can explain why some synapses show depression and others show facilitation at low to intermediate stimulation frequencies. Multistep priming also suggests a mechanism for frequency invariance of steady-state release, which can be observed in some synapses involved in sensory processing.

Introduction

Quantitative analysis of neurotransmitter release has its roots in the early work of Sir Bernhard Katz and collaborators. Studying the stochastic nature of quantal release of acetylcholine at the neuromuscular junction, they noticed that the statistics of release is not quite compatible with the expectation for mutually independent release of synaptic vesicles (SVs) from an unlimited reservoir. Rather, they concluded that their data can best be described by a binomial distribution. Thus, they argued that there must be a limiting resource of SVs, which prevents statistical fluctuations of release from being larger than what they called the number of "units available," and introduced the concept that release is proportional to the total number of available units, n, and a mean probability of release, $\bar{p}$, of such units (Del Castillo and Katz, 1954). Originally, n was assumed to be constant and often referred to as the readily releasable pool (RRP) of SVs (but see notable exceptions, such as Worden et al. [1997], Vere-Jones [1966], and Quastel [1997]). The classical studies on the kinetics of release and its role in short-term plasticity (STP) up to 2002 have been extensively and competently reviewed by Zucker and Regehr (2002). The priming process is seen as the tethering and docking of SVs to specialized release sites, as well as the build-

up of macromolecular complexes, which mediate Ca^{2+}-dependent triggering of exocytosis. Priming occurs on the tens of milliseconds to seconds timescale, while action potential (AP)-triggered SV fusion happens within tens to hundreds of microseconds.

Classical release models often assumed a homogeneous pool of primed SVs, limited by the number of release sites, which is assumed to be constant during the time of a typical electrophysiological experiment (tens of minutes). Many classical studies assumed priming to be a one-way process, such that in the absence of stimulation, eventually all release sites fill up with SVs. Consequently, the resting RRP has a fixed size, equal to the number of release sites (Liu and Tsien, 1995; Dittman and Regehr, 1998; Hallermann et al., 2010). Recently, however, evidence has been accumulated that the priming process is dynamic and reversible, such that the RRP may fluctuate in size, and even at rest a significant fraction of release sites may remain empty (reviewed by Neher and Brose [2018]). Indeed, variance–mean analysis of glutamatergic transmission at cerebellar parallel fiber to molecular layer interneurons showed that only about 45% of release sites are occupied at rest (Miki et al., 2016; Malagon et al., 2020). Further electrophysiological evidence demonstrated that synapses may transiently overfill the RRP beyond

[1]Max Planck Institute for Multidisciplinary Sciences, Göttingen, Germany.

Correspondence to Erwin Neher: eneher@gwdg.de.

its resting state after high-frequency activity (Junge et al., 2004) and that the expression of a particular combination of synaptic proteins, comprising at least one isoform of CAPS, Munc13-1, and Munc18-1, is favorable for establishing a large stable pool at rest (Jockusch et al., 2007; He et al., 2017). Correspondingly, electron tomography demonstrated that a similar combination of proteins is required for the presence of tightly docked SVs at active zones (Imig et al., 2014). Using high-pressure quick-freeze technology together with precisely timed stimulation of synapses, it could be demonstrated that in spite of consumption of release-ready SVs during stimulation, the number of tightly docked SVs increases shortly after stimulation and reaches a peak when quick-freezing is performed about 10 ms after stimulation. However, this increase is only transient and decays back to baseline within about 100 ms (Watanabe, 2016; Chang et al., 2018; Kusick et al., 2022). Using in vitro secretion assays, Prinslow et al. (2019) demonstrated that partially assembled molecular complexes are prone to disassembly by the action of NSF. Together with mutagenesis studies of Munc13, these findings have led to a molecular scheme of step-wise and reversible buildup of the release machinery with a pivotal role of Munc13 and its regulatory domains (Neher and Brose, 2018; Dittman, 2019).

Several recent electrophysiological studies have accommodated such evidence by proposing a two-step priming process under the restrictive assumption of only one fully mature state of the release machinery, which is release-competent (Doussau et al., 2017; Miki et al., 2018; Pulido and Marty, 2018; Bornschein et al., 2020; Kobbersmed et al., 2020; Lin et al., 2022; Weingarten et al., 2022). These models thus recapitulate the step-wise assembly and maturation of the release machinery, as discussed above. Numerical simulations based on such priming schemes are capable of reproducing a variety of electrophysiological findings. In reference to the results from electron tomography, the two states in question may be called "loosely docked" (LS) and "tightly docked" (TS) (Neher and Brose, 2018). It is an open question, however, whether the postulated functional states of the model actually correspond to the two morphologically defined states or else represent some other steps in the buildup of the molecular release machinery.

Alternatively, kinetic models have been developed, which assume that SVs migrate between or dock at different release sites (Grande and Wang, 2011), from which release occurs in parallel with different release probabilities, p_r (high and low), and different priming rates (fast and slow) (Hallermann et al., 2010; Delvendahl et al., 2013; Mahfooz et al., 2016). Many electrophysiological findings, including biphasic depression and recovery kinetics, can readily be explained both by parallel and sequential models. It is obvious, though, that molecular interpretations of such features, as well as of the changes observed after genetic or pharmacological manipulations, may differ substantially. Specifically, many features, which on the basis of parallel or classical single-pool models are explained as differences and variations in release probability, can very well also be explained assuming constant release probability combined with changes in the resting equilibrium and dynamics between priming states (Pulido and Marty, 2018; Lin et al., 2022). In the

following one variety of a sequential model, the LS/TS model (Neher and Brose, 2018; Lin et al., 2022) is shortly explained and a few examples are given for differences in the interpretation of published data when viewed in terms of classical pool models or else as a reversible sequence of priming steps during the buildup of a fully functional release machinery.

The two-step sequential priming scheme

As detailed above, the kinetic scheme of the LS/TS model was inspired by the finding that the priming process is reversible (Smith et al., 1998; Murthy and Stevens, 1999; He et al., 2017) and by the evidence from electron microscopy that under conditions of intact priming a subset of SVs near the plasma membrane is tightly docked within 2 nm distance (Imig et al., 2014; Maus et al., 2020). Considering such findings, Neher and Brose (2018) proposed a model (Fig. 1 A) with a fixed number, N, of release sites, which at any given time can either be empty (state ES) or occupied by an SV in one of two states: the TS state or the LS state. The model furthermore assumes that docked vesicles can reversibly change states with rate constants in the forward priming direction, k_1 and k_2, being accelerated by activity (and more specifically by cytosolic [Ca^{2+}]) and with backward rate constants b_1 and b_2 (Fig. 1, A and B). The latter were assumed to be constant for simplicity. Importantly, SV fusion was allowed to occur only from the fully primed state TS with a probability (per AP) of p_{fusion}. Surprisingly, short-term plasticity patterns recorded at the calyx of the Held synapse in response to stimulation up to 20 Hz could be simulated by this relatively simple kinetic scheme (Lin et al., 2022). As described in more detail below in the context of short-term depression and frequency-invariant transmission, the assumption of priming rates linearly increasing with cytosolic [Ca^{2+}] leads to a particularly simple scenario with a plateau in the relationship between the level of synaptic depression and stimulation frequency in the range 5–20 Hz.

For higher frequencies (>20 Hz), three observations require extensions of the model: (1) the steady-state quantal content of release declines progressively with increasing frequency, reflecting limitations of vesicle supply; (2) many synapses exhibit prominent paired-pulse facilitation (PPF); and (3) p_{fusion} increases, in part due to Ca^{2+}-current facilitation (Borst and Sakmann, 1998; Cuttle et al., 1998; Müller et al., 2008; Lin et al., 2012). The first observation, a limited rate of supply of SVs, can conveniently be implemented by assigning a Michaelis–Menten type saturation to the Ca^{2+}-dependence of one or both of the forward priming rate constants. Alternatively, so-called "release-site clearing" may be introduced as a process limiting the rate of SV supply. In that case, a site being vacated by SV fusion is assumed to reside in a refractory state for a certain time before being able to accept a new vesicle (state "ERS," Fig. 1 C). The second feature, PPF observed at frequencies ≥50 Hz, depends on several aspects of the model (see below). In particular, it requires an extension, which specifically simulates the discovery by electron tomography of a transient increase of tightly docked SVs after APs. This transient tight docking lasts for about 50–100 ms (Kusick et al., 2022), which is similar to the time of decay of PPF (Chang et al., 2018). It is implemented in the
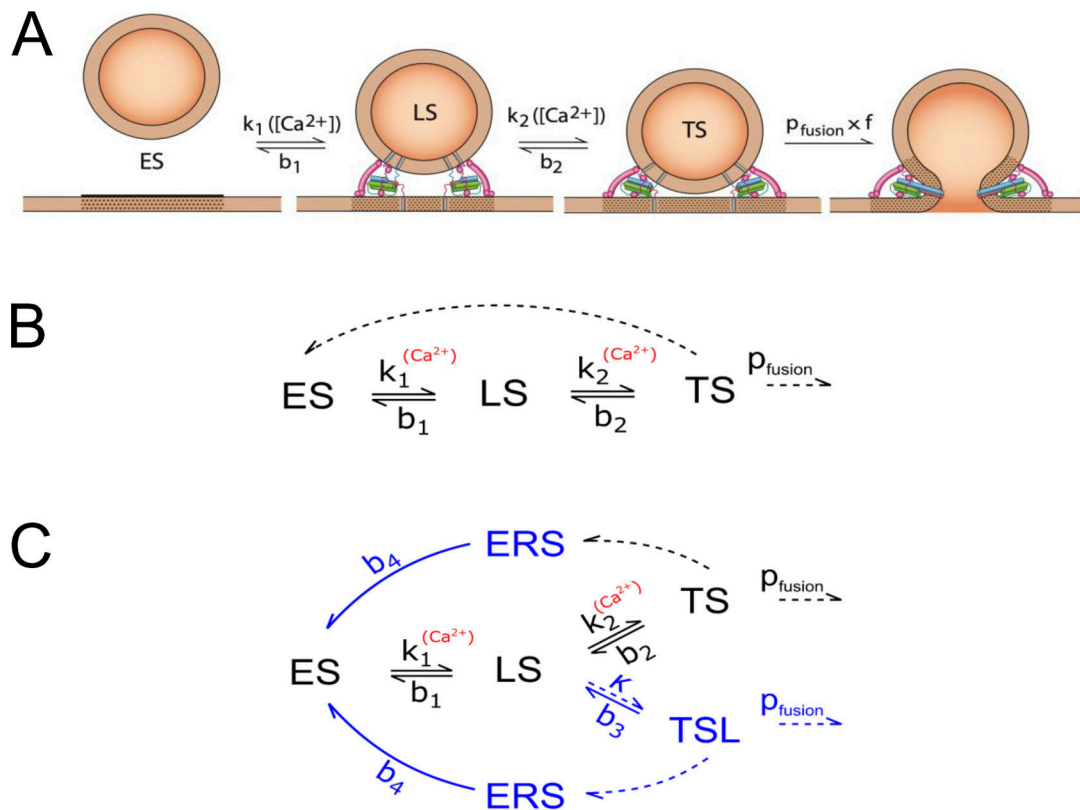
Figure 1.   **Schematic representation and kinetic scheme of the LS/TS model. (A)** Graphical representation. A release site can either be empty (state ES) or else occupied by a vesicle in a LS state or a TS state. Only vesicles in TS can be released during an AP with release probability p_{fusion}. Transitions between states are characterized by rate constants $k_1([Ca^{2+}])$, $k_2([Ca^{2+}])$, b_1, and b_2 (modified from Neher and Brose [2018]). **(B)** Kinetic scheme of the simple model, which is valid for frequencies <50 Hz and reproduces the plateau in the relationship between steady-state release and stimulation frequency. At higher frequencies steady-state release drops, which can be simulated by using a Michaelis–Menten type saturation of the priming rate constant k_1. **(C)** To simulate PPF and to recapitulate the Flash and Freeze findings, it was necessary to add TSL, a labile TS state. TSL is release competent, just like TS, the main difference between TS and TSL is an ∼50-fold faster backward rate constant, b_3, as compared to b_2. Thus, SVs entering TSL after an AP will rapidly fall back to LS and contribute only little to release during a subsequent stimulus unless ISIs are <20–50 ms. Therefore, TSL vesicles are "invisible" for frequencies <20 Hz. The extended scheme also includes an alternative for simulating the decrease of steady-state release at high frequencies. Instead of becoming immediately available for vesicle docking, vacated release sites transiently adopt an empty refractory state (ERS), from which they return to ES with a rate constant b_4 (modified from Lin et al. [2022]).

model as a fusion-competent "labile tight state" (TSL; Fig. 1 C; Lin et al., 2022). TSL vesicles are assumed to have the same p_{fusion} as TS vesicles but transition back to LS with a rate constant much faster than the backward rate constant b_2 by which the TS vesicles convert back to LS (see more details in the paragraph of PPF, below).

The LS/TS model is not only able to reproduce several experimentally observed aspects of short-term plasticity quite faithfully but it can also account for the large heterogeneity in synaptic strength which is observed at the calyx of Held and several other glutamatergic synapses (typically varying over a factor of 10). By means of varying the relative abundance of fully primed TS vesicles in resting synapses, the LS/TS model offers a potent mechanism for adjusting synaptic strength without the need to postulate changes in release probability and total number of release sites. Similar conclusions were reached by Pulido and Marty (2018) using a slightly different two-step priming model. Furthermore, incompletely primed, but docked vesicles were recently postulated for hippocampal synapses between CA1 pyramidal cells and oriens lacunosum-moleculare (O-LM) interneurons by Aldahabi et al. (2022).

Estimates of pool size and release probability

Before discussing changes in pool size and release probability, as observed during experimental manipulations, some clarification is required regarding the methods that are commonly used for the estimation of these quantities.

Most traditional methods of quantal analysis implicitly assume the classical model of a single homogenous RRP (see Neher [2015] and Thanawala and Regehr [2016] for review). Common to these methods is the application of a strong stimulus (high-frequency train of APs, hypertonic stress, or direct presynaptic depolarization under voltage-clamp) to deplete the RRP within a time short enough, such that pool replenishment during the stimulus is negligible, or else can be corrected for. The RRP is then calculated as the replenishment-corrected cumulative release. Subsequently, a quantity commonly termed release fraction (F), fusion efficiency (f_e), or vesicular release probability (p_{vr}) can be obtained as the fraction of the RRP released by a single AP. For a parallel model, assuming two or more subpools of fusion-competent SVs, this fraction represents an average of release probabilities of contributing subpools, weighted by the

respective subpool sizes at rest. For the sequential (LS/TS) model, this fraction reports the "true" release probability (p_{fusion}) of TS vesicles only, if the RRP estimate corresponds to just the TS subpool. However, modeling of data obtained from the calyx of Held synapses indicates that typical pool-depleting stimuli deplete both the LS and TS subpools (as discussed in Lin et al. [2022] and Neher and Taschenberger [2021]). Thus, the quantity reported as RRP is the sum of LS and TS subpools present at stimulation onset, and the fraction of the RRP released by a single AP represents an apparent release probability, which depends on the ratio of subpool sizes. Correspondingly, changes in apparent release probability upon molecular perturbations may well represent changes in the LS/TS ratio at constant p_{fusion}. Thus, a role in the process of SV fusion might be erroneously assigned to a protein under study.

Alternative methods

The analysis of mean and variance of quantal release, elicited by repetitively applied stimuli, is often used to determine RRP size, the number of release sites, N, and release probability (Silver, 2003). For a homogeneous vesicle pool of size N, which refills completely in pauses between individual trials, variance is given by $\sigma^2 = N \cdot q^2 \cdot p_r \cdot (1 - p_r)$, where q is the quantal size and p_r is the probability of release. A plot of variance versus mean, measured under several different conditions, such as different concentrations of extracellular Ca^{2+}, can be fitted by a parabola. This curve starts near the origin with low values of both mean and variance from measurements at low $[Ca^{2+}]$ with small p_r. With increasing p_r, variance reaches a maximum at $p_r = 0.5$ and subsequently decreases due to the term $(1 - p_r)$ in the equation for variance. The parabola approaches 0 when p_r approaches 1, which means that there are no more trial-to-trial fluctuations since the same number of SVs ($= N$) is released at each trial. The intersection of the parabola with the abscissa is therefore given by the product of N*q. Quantal amplitude, q, is given by the initial slope of the parabola. Thus, the number of release sites, N, can be calculated. Importantly, this holds under the assumption of a single homogeneous pool, which fills up completely between stimuli.

However, for reversible and dynamic priming, responses fluctuate even for $p_{fusion} = 1$ due to the stochastic nature of the priming process. Thus, p_r in the equation for variance has to be replaced by the product of p_{fusion} and $p_{occupancy}$, where $p_{occupancy}$ represents the fraction of release sites occupied by fusion-competent SVs (Vere-Jones, 1966; Quastel, 1997; Scheuss and Neher, 2001). Therefore, the parabola in its descending part approaches 0 only when both p_{fusion} and $p_{occupancy}$ approach the value of 1. This is the case only when at the time of stimulation almost all sites are occupied ($p_{occupancy} = 1$) and all fusion-competent SVs are released ($p_{fusion} = 1$). Unfortunately, such conditions are difficult to obtain (Malagon et al., 2020), requiring the strongest stimulation and conditions of enhanced priming. In addition, saturation and desensitization of postsynaptic receptors may distort the descending branch of the parabola (Meyer et al., 2001) unless quanta can be counted directly, as is the case for some types of synapses in the cerebellum (Malagon et al., 2020; Silva et al., 2021) and hippocampus

(Tanaka et al., 2021). As a consequence, the parabola may include unreliable data points on its descending branch and the extrapolation toward the intersection with the abscissa may be inaccurate. Provided N can be estimated reliably, one can calculate p_r for a given condition as the fraction of N released by a single stimulus. However, there is still the problem of splitting p_r into its factors p_{fusion} and $p_{occupancy}$, which is not possible on the basis of mean and variance alone.

In the absence of readily available methods to separate priming and fusion by statistical methods, several procedures have been described to address the multiplicity of pools and functional states directly. Next for optimization of model fits, assuming pools with different topologies and kinetics (Hallermann et al., 2010; Delvendahl et al., 2013; Doussau et al., 2017) special properties of postulated subpools have been exploited to determine their properties. For instance, the assumption of a subpool of "superprimed" SVs with high release probability, dependent on the presence of at least one isoform of Rab3, has been used for its isolation by subtraction of responses recorded in synapses of quadruple Rab3 knockout mice from those recorded in control synapses (Schlüter et al., 2004). Subtraction of control responses from those measured after induction of LTP has been used to demonstrate that LTP increases a component of release with high p_{fusion} and slow recovery kinetics (Weichard et al., 2023). Special statistical properties of so-called "pre-primed" SVs have been used to estimate their contribution to overall release at hippocampal synapses (Gustafsson et al., 2019). Likewise, the contribution of SVs occupying "docking sites," as opposed to those occupying "replacement sites," has been estimated by detailed model fitting and statistical analysis of quantal responses to repetitive, high-frequency stimulation (Miki et al., 2016, 2018; Silva et al., 2021). A variant of the technique of non-negative tensor factorization (NTF) has been developed to determine the release probability of TS vesicles in a way that is consistent with the LS/TS model and with the variation of synaptic strength between synapses (Neher and Taschenberger, 2021; Lin et al., 2022).

Unfortunately, it is still unproven whether any of these approaches allow an unambiguous separation between the effects of a given manipulation on vesicle priming from those on vesicle fusion or else an unequivocal differentiation between parallel and sequential models. However, as pointed out by Miki et al. (2016), variance analysis of cumulative release at cerebellar synapses is more readily explained by sequential than by parallel models. Nevertheless, one should be aware that alternative interpretations are possible, which lead to quite different conclusions in terms of molecular mechanisms when either a parallel or else a sequential scheme is assumed. Some examples will be discussed here.

Redistribution of synaptic efficacy—A change in release probability or priming?

Markram and Tsodyks (1996) studied changes in STP following the induction of presynaptic LTP in layer 5 neocortical synapses. They observed that single EPSPs were potentiated significantly. However, the sum of EPSPs during short bursts of activity was hardly changed because the increase in the first EPSP of a burst

was compensated by decreases in subsequent EPSPs. They called this phenomenon "Redistribution of Synaptic Efficacy" and pointed out its high relevance for information processing since APs occur often in short bursts in the brain area studied.

Standard quantal analysis within the classical model can readily explain this finding by assuming a change in release probability and a limited RRP, which is full at rest and refilled relatively slowly. In this scenario, presynaptic AP bursts would progressively empty the RRP and this would happen faster at a higher release probability such as after induction of LTP. The first response would be larger and subsequent ones smaller due to the limitation of RRP sizes. Thus, a reasonable conclusion from these findings is that induction of this kind of presynaptic LTP causes an increase in release probability. One might therefore argue that this change is primarily mediated by proteins regulating exocytosis, such as SNAREs, synaptotagmin 1 and 2, Ca^{2+} channels, and/or affecting the coupling of Ca^{2+} channels to release sites.

However, as shown by Lin et al. (2022), a shift in the balance between LS and TS subpools at rest in favor of the latter might equally well cause the observed redistribution of synaptic efficacy, resulting in larger initial amplitudes and faster fatigue of responses during bursts. As suggested before (Neher and Brose, 2018), such a shift may well be caused by the priming protein Munc13, the function of which is regulated by second messengers such as $[Ca^{2+}]$, diacylglycerol, and phosphoinositides. Thus, considering two-step priming schemes opens up completely different options for interpretation. In fact, a recent study by Weichard et al. (2023) could describe changes in synaptic strength and STP following LTP induction equally well with release models based on either parallel or sequential priming schemes. Importantly, increased synaptic strength and slower recovery from synaptic depression following LTP induction were found to arise primarily from a larger proportion of fully primed slowly recovering SV in the absence of a change in release probability.

Diversity in synaptic strength

Synaptic strength of glutamatergic synapses of a given type often varies by about an order of magnitude (Harris and Stevens, 1989; Debanne et al., 1996; Dobrunz and Stevens, 1997; Losonczy et al., 2002; Taschenberger et al., 2016). Presynaptic parameters contributing to this heterogeneity may of course be differences in the size and morphology of terminals, giving rise to varying numbers of active zones and release sites (Harris and Stevens, 1989; Grande and Wang, 2011). Very often synaptic strength is negatively correlated with "paired pulse ratio" (PPR), the ratio of second over first responses to a pair or burst of stimuli. A change in PPR is generally considered an indication of a change in release probability. Thus, as in the case of induction of LTP discussed above, differences in PPR between synapses may well be interpreted as differences in release probability. However, as shown by Lin et al. (2022), this feature can again be explained by variation in the TS/LS ratio at rest. In this context it should be noted that Munc13, a prime candidate for regulation of the TS/LS ratio (Betz et al., 1998; Rhee et al., 2002; Junge et al., 2004; Shin et al., 2010; Neher and Brose, 2018; Dittman, 2019; Rizo,

2022), is expressed in at least two isoforms in the brain, which may confer different degrees of stability to vesicles in the fully primed state (Rosenmund et al., 2002; He et al., 2017), but see Holderith et al. (2022). Thus, rather than differences in the release mechanism, differential expression of isoforms of priming proteins might be the cause of the diversity of synaptic strength among synapses of one type, between synapses of different types, or after activity-induced long-term changes in synaptic strength including LTP and LTD (Weichard et al., 2023). Furthermore, Munc13 has regulatory binding sites for $[Ca^{2+}]$, calmodulin, and diacylglycerol (Betz et al., 1998; Rhee et al., 2002; Lipstein et al., 2013), providing options for regulation spanning a time range from milliseconds to hours and days (Tewson et al., 2012; Kruse et al., 2016; Schuhmacher et al., 2020). The distribution of synaptic strengths may well reflect the history of modulatory influences, both long- and short-term, that a given synapse was exposed to.

It should be noted that in the classical view of a single homogenous vesicle pool and a non-reversible priming process, only the number of release sites and the release probability can be invoked as presynaptic parameters describing diversity in synaptic strength since all release sites will eventually be fully occupied at rest. Reversibility of vesicle priming allows for partial occupancy of release sites at rest and, therefore, provides options for dynamic changes in both directions, facilitatory and depressing (Pulido and Marty, 2018). The repertoire of modulatory influences on neurotransmitter release is thus expanded, possibly comprising the whole range of second messenger-mediated signaling.

Short-term depression at low frequencies

Depression of synaptic responses during train stimulation can have pre- and postsynaptic causes (Zucker and Regehr, 2002). Depletion of the RRP due to limited resupply of readily releasable vesicles is generally considered to be the most relevant presynaptic contribution to depression (Elmqvist and Quastel, 1965; Betz, 1970; Rosenmund and Stevens, 1996; Tanaka et al., 2021). During repetitive stimulation, the response amplitude reaches a steady state that represents the balance between the mean release rate (the product of release probability, stimulation frequency, and remaining RRP) and the mean rate of vesicle resupply. Notably, it was often found that the rate of resupply necessary to account for the observed steady-state release during stimulation was substantially higher than that estimated from the time course of recovery of the RRP after stimulation. Thus, it was postulated that the vesicle priming rate must be higher during stimulation than during recovery at rest. Ca^{2+}-dependent enhancement of vesicle supply was therefore postulated (Dittman and Regehr, 1996; Stevens and Wesseling, 1998; Wang and Kaczmarek, 1998; Dittman et al., 2000; Hosoi et al., 2007; Hallermann and Silver, 2013; Mahfooz et al., 2016; Weingarten et al., 2022). Recent studies suggest synaptotagmin 3 (Weingarten et al., 2022), synaptotagmin 7 (Liu et al., 2014; Chen et al., 2017; Tawfik et al., 2021; Kusick et al., 2023), and the C2B domain as well as the calmodulin-binding domain of Munc13 (Lipstein et al., 2013, 2021) to be candidates for the Ca^{2+}-sensor mediating this type of stimulus-dependent enhancement of the priming process. The Ca^{2+}-dependence of the resupply of
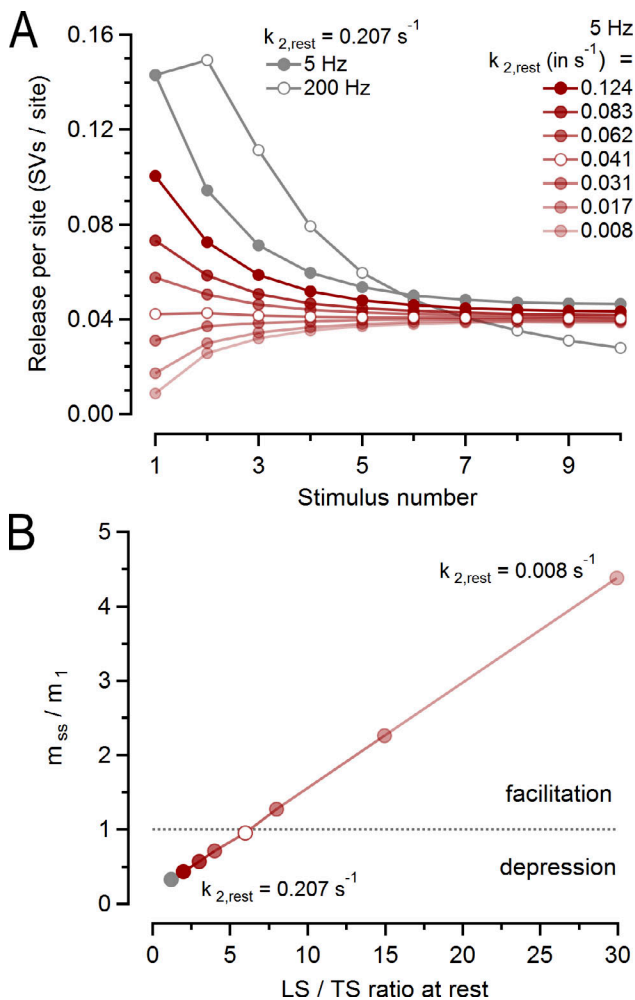
Figure 2. Activity-dependent enhancement of priming as a mechanism regulating depression and frequency facilitation. (A) Numerical simulations for 5 Hz stimulus trains (gray and red dots). Release from a single site is plotted against the stimulus number. Model parameters were similar to those as published by Lin et al. (2022), except for one parameter ($k_{2,rest}$, the resting value of k_2), which was varied between 0.207 s^{-1} (the value for calyx data; gray dots) and 0.0083 s^{-1} (red dots) in order to achieve different degrees of TS occupancy at rest. The respective values for $k_{2,rest}$ are indicated to the right. Release time courses show depression or facilitation depending on the choice of $k_{2,rest}$. The transition from depression to facilitation occurs at a value of $k_{2,rest}$ = 0.044 s^{-1} (priming events per site and second) at which the occupancy of TS at rest is equal to occupancy at steady state (red circles). The steady-state release, m_{ss}, changes only a little when changing the resting model parameters while the initial release during train stimulation is strongly dependent on these parameters. The model predictions for a 200 Hz train, according to Lin et al. (2022), are shown for comparison (gray circles). **(B)** Plot of steady-state quantal content, m_{ss}, divided by initial quantal content, m_1, against the LS/TS ratio at rest. Similar plots, demonstrating variations in depression and facilitation upon changing resting parameter values, can be generated by increasing b_1 or b_2 or else or else by decreasing $k_{1,rest}$.

release-ready SVs may lead to biphasic recovery from depression if stimulus trains elicit long-lasting increases in presynaptic residual [Ca^{2+}].

Biphasic depression and recovery time courses, typically observed at various glutamatergic synapses, have been simulated by models assuming two populations of vesicles or release

sites (parallel model): a high-p population with slow priming and a low-p population with fast priming (Ritzau-Jost et al., 2018). However, the LS/TS model with only a single type of release site can also reproduce all aspects of depression and its recovery studied at the calyx of Held (Lin et al., 2022). The model assumes forward priming rate constants to be described by the sums of their basal values at rest plus components, which rise linearly with cytosolic [Ca^{2+}]. This allows one to distinguish two frequency ranges for describing responses to repetitive stimulation: a low-frequency range (0.1–2 Hz) in which steady-state release is determined by both forward and backward transitions and a mid-frequency range (5–20 Hz) in which forward transitions dominate over backward transitions. In the low-frequency range, steady-state release decreases with increasing frequency because vesicle resupply during long interstimulus intervals (ISIs) is primarily determined by the basal rate constants at rest. Resupply is less for shorter ISIs (higher frequencies). In the mid-frequency range, however, basal priming during short ISIs is negligible in comparison to the accelerated priming during AP-induced Ca^{2+} transient. Each transient shifts certain fractions of SVs from their pre-AP state to the corresponding downstream state depending on the time integral over the Ca^{2+} transient and the steepness of the Ca^{2+}-dependence of priming. The fractions transferred between the first and second priming steps will be referred to as s_1 and s_2 in the following. Provided that AP-induced Ca^{2+} transients do not summate significantly in this frequency range, APs act nearly "autonomously," advancing such fractions of SVs irrespective of the ISI duration. Likewise, p_{fusion} is constant in this range of stimulation frequencies. This results in steady-state levels of site occupancies, which are almost independent of frequency since both release and resupply increase nearly linearly with stimulation frequency. Steady-state release then depends mainly on three parameters: s_1, s_2, and p_{fusion} (Lin et al., 2022). Model synapses display depression or facilitation at low frequencies depending on whether their steady-state TS occupancy is lower or higher than resting TS occupancy. The latter is determined by four other model parameters, namely the resting values of forward and backward priming rate constants ($k_{1,rest}$, $k_{2,rest}$, b_1, and b_2). Thus, one can adjust TS occupancies at rest and at steady-state independently from each other, a consideration that will be relevant when discussing facilitation at low frequencies and frequency-invariant transmission below.

At the calyx of Held, the plateau level of steady-state synaptic depression is located at about 35% of the initial EPSC (see Fig. 2 A and Fig. 3 A, gray traces). Thus, these synapses display depression in the low-frequency range. At frequencies >20 Hz, the steady-state release per AP deviates from the midfrequency plateau declining progressively due to a saturation of vesicle supply (see below).

Frequency facilitation (FF)

Some types of synapses show facilitation instead of depression at low frequencies, often referred to as FF or augmentation (Zucker and Regehr, 2002). Common to these types of short-term plasticity is a very large dynamic range (an increase up to 10-fold) and an onset already at stimulation frequencies as low as 1 Hz
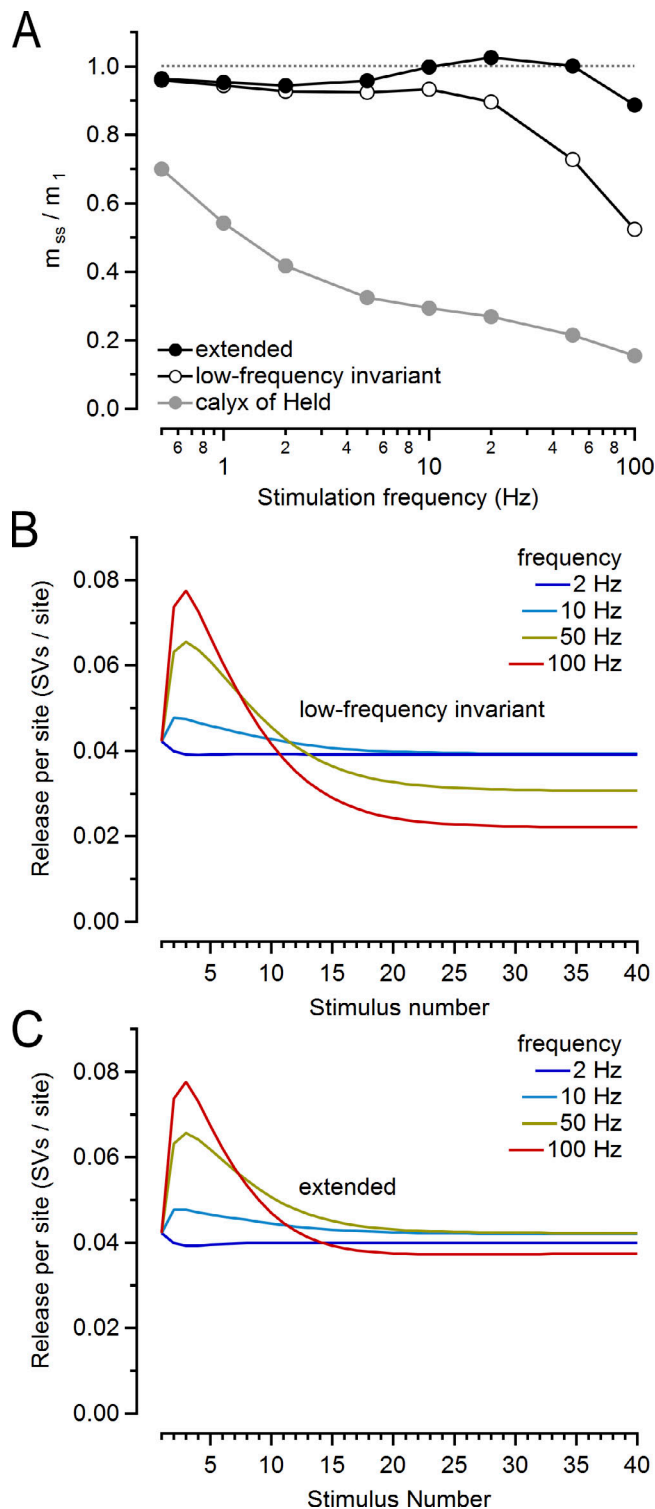
A

B

C

(Toth et al., 2000; Nicoll and Schmitz, 2005; Chamberland et al., 2014; Midorikawa and Sakaba, 2017). At intermediate frequencies (10–100 Hz) and low extracellular [Ca²⁺], FF is hard to distinguish from PPF, another type of facilitation to be described below. Therefore, the two types of facilitation are often conceived together as short-term facilitation. Implicitly, the same "Ca²⁺-sensor" is assumed to mediate Ca²⁺ sensitivity (Jackman et al., 2016). The two-step priming scheme, however, suggests a very different mechanism for facilitation in the frequency of 1–20 Hz in comparison with that at 100–200 Hz. As detailed above, the LS/TS model, as applied to the calyx of Held data, predicts that steady-state release is relatively constant during repetitive stimulation at 5–20 Hz and that this synapse shows depression since the resting occupancy of TS is higher than that at steady state. The model prediction of depression can readily be converted into facilitation by assuming a lower occupancy of the TS state at rest. Consequently, the first EPSC in a stimulus train will be small. During the train, release will increase toward the steady-state level, as determined by parameters s_1, s_2, and p_{fusion}. Fig. 2 A (red traces) shows predictions for release time courses in response to 5 Hz stimulation for different relative occupancies of TS at rest. Note that all release time courses are calculated using the same $p_{fusion} = 0.39$, which was assumed to be constant throughout trains. Individual traces start at different initial quantal content (m_1) depending on the chosen value for $k_{2,rest}$ and converge toward similar steady-state quantal contents (m_{ss}). It turns out that a value of 0.044 (priming events per site and second) for the priming rate constant $k_{2,rest}$ results in the release that is almost constant during the entire stimulus train (Fig. 2 A; open circles). Fig. 2 B shows the ratio "steady-state release over first release" as a function of the LS/TS ratio. It is seen that "facilitation," defined this way, reaches high values for LS-dominated synapses (large LS/TS ratio), whereas this ratio is <1 for TS-dominated synapses. In this sense, facilitation and depression at low frequencies reflect the same process and FF may be considered "negative depression," not involving changes in p_{fusion}.

Models for FF with similar "stimulus-dependent mobilization" were actually proposed by Worden et al. (1997) and Pan and Zucker (2009) for describing this phenomenon at the lobster neuromuscular junction. FF at cerebellar granule to Purkinje cell synapses (Doussau et al., 2017) was also postulated to be the result of a stimulus-dependent shift between two states of priming. The important point, shown in Fig. 2, is that one can

Figure 3. Frequency-invariant steady-state transmission. (A) Depression (steady-state release divided by first release) as a function of stimulation frequency. At the calyx of Held, synaptic depression is already observed at low frequencies (0.3–5 Hz). Between 5 and 20 Hz, depression displays a plateau, while release further declines at 50 Hz and higher. Such behavior is reproduced by the model parameters as used in Lin et al. (2022) (gray dots). At low frequencies, invariant-type of depression can be achieved by using the same model parameters, except for $k_{2,rest}$, which was changed here to the value of 0.044 s⁻¹, resulting in a near-constant quantal content during a 5 Hz stimulus train (compare Fig. 2 A). This parameter choice led to near-constant

m_{ss}/m_1 over a large range of stimulation frequencies up to 20 Hz (empty black circles, trace 'low-frequency invariant'). Increasing the model parameter, which controls saturation of priming in terms of a Michaelis–Menten process by a factor 3 further extends the range of near-constant m_{ss}/m_1 up to 100 Hz (filled black circles, trace 'extended'). **(B)** Model synapses with frequency-invariant steady-state release show dynamic STP. Release versus stimulus number is shown for four frequencies (2, 10, 50 and 100 Hz). Model parameters are identical to those of the 'low-frequency invariant' trace in panel A. Traces for 50 and 100 Hz show transient facilitation and late depression. **(C)** Enhancing release at high frequencies by reducing the effect of priming saturation (same parameters as 'extended' trace in panel A) reduces late depression and results in release time courses displaying early facilitation and a nearly frequency-invariant late phase.

change a model of low-frequency depression, as observed in the calyx of Held, into one for FF by just changing one parameter, the resting rate constant of priming. In this view, the Ca^{2+} sensor for FF is the same as the one that enhances priming at elevated cytosolic $[Ca^{2+}]$, candidates for which are Munc13 (Lipstein et al., 2021), synaptotagmin 7 (Turecek and Regehr, 2018), and/or synaptotagmin 3 (Weingarten et al., 2022). Enhancement of p_{fusion} is not required for simulating FF at low frequencies.

Frequency-invariant synaptic transmission

The calyx of Held, a synaptic terminal in the auditory pathway, is often considered a simple one-to-one relay for converting presynaptic into postsynaptic spike trains, irrespective of frequency. This was shown to be actually the case for calyx synapses of adult mice (Lorteije et al., 2009). Such frequency invariance is also observed in some other types of synapses involved in sensory signal processing and motor control (MacLeod et al., 2007; Bagnall et al., 2008; Turecek et al., 2016, 2017). Synaptotagmin 7 is required to obtain frequency invariance in these synapses through a facilitating mechanism compensating for short-term depression (Turecek et al., 2017). In contrast to the situation for adult animals, these synapses and the calyx of Held synapse display pronounced short-term depression during early development, which gradually diminishes with age. For P13–P15 calyx synapses, which is the developmental stage studied by Lin et al. (2022), a plateau region is observed in the relationship between steady-state synaptic strength and stimulation frequency (see above and Fig. 3 A, trace calyx of Held). It may be speculated that this plateau is an early sign of frequency invariance, as it develops. If so, the mechanism discussed above in the context of depression and frequency facilitation may give a hint on how synapses can achieve frequency invariance over a wider frequency range.

Parameters for the resting occupancy of TS can be chosen in ways that the plateau level of release is approached during a stimulus train either from above (depression) or from below (FF; see above). Likewise, parameters can be chosen to obtain an initial release matching the plateau level. Then TS-occupancy and steady-state release are frequency invariant from very low frequencies up to 20 Hz without the need to invoke a balance between changes in p_{fusion} and those in priming (see Fig. 3 A, trace 'low-frequency invariant'). At the high-frequency end, the simple model, as discussed so far, has to be extended by several features, such as a rise in p_{fusion}, saturation of vesicle priming, and release from a labile tight state, TSL (see above and the section on PPF). Such effects dominate steady-state release at a frequency >50 Hz. Thus, one can conceive several mechanisms on how to extend the range of frequency invariance to higher frequencies, for instance by reducing saturation of priming (see Fig. 3 A, trace 'extended' for an example). This change extends the frequency range of near-constant steady-state release up to 100 Hz with remaining variations confined to about ±10%. Importantly, such adjustments involve changes in p_{fusion} only for the highest frequencies (100 and 200 Hz). In contrast frequency invariance at synapses for sensory signal processing and motor control was explained as a balance between depression and facilitation, the latter being simulated as an increase in release probability (Turecek et al., 2017).

In spite of the constancy of steady-state release over a wide frequency range, the model proposed here does predict dynamic changes in release during high-frequency trains or when abruptly changing frequency. Fig. 3, B and C, shows examples for such time courses. Similar transient dynamic changes were also reported for frequency-invariant synapses between Purkinje cells and deep cerebellar nuclei and vestibular synapses (Turecek et al., 2017).

Paired-pulse facilitation (PPF)

PPF, as discussed here, is one of the most studied forms of facilitation. It can be observed during pairwise stimulation at short interstimulus intervals in many types of glutamatergic synapses (Atluri and Regehr, 1996; Zucker and Regehr, 2002) and also at the neuromuscular junction (Katz and Miledi, 1968). Typically, only the second and/or third response in a stimulus train is augmented and subsequent responses diminish rapidly. The same types of synapses often show pronounced depression at lower frequencies (Varela et al., 1997; Sun et al., 2005). At the calyx of Held, indications of PPF are observed in a fraction of synapses, if stimulated at frequencies ≥50 Hz (Lin et al., 2022; see Fig. 2 A, gray trace, open circles). The extent of PPF strongly depends on residual Ca^{2+}. Several studies, therefore, tried to identify "the Ca^{2+}-sensor" of PPF (Zucker and Regehr, 2002; Jackman et al., 2016), often assuming that this sensor, when Ca^{2+}-bound, enhances release probability. However, in the framework of the LS/TS model in its extended form (Lin et al., 2022), Fig. 1 C, PPR depends on the interplay of at least four factors (Lin et al., 2022):

(1) Depletion of the RRP by the release during the first stimulus depending on p_{fusion}.
(2) Facilitation of presynaptic Ca^{2+}-current (Borst and Sakmann, 1998; Müller et al., 2008), increasing p_{fusion} of the second response.
(3) Ca^{2+}-dependent enhancement of vesicle replenishment (depending on s_2).
(4) A transient boost of replenishment of fusion-competent SVs by the labile state, TSL.

Three of these factors contribute to an increase in the second response in a pair of stimuli, while the first factor counteracts such facilitation. The labile state (TSL; Fig. 1 C) was introduced to simulate the transient docking of SVs after an AP, as observed by "flash and freeze" electron microscopy (Kusick et al., 2022). Its contribution to release was found to be essential for an adequate simulation of PPF as observed at the calyx of Held synapses (Lin et al., 2022). Specifically, about half of the depletion of the RRP due to release is compensated by the recruitment of TSL vesicles, which transiently contribute to the release of the second, but not to that of the first stimulus in a train. The full contribution of TSL vesicles is obtained only for frequencies of 100 Hz and higher, given the assumption of the model that the increase of tightly docked SVs after an AP is transient and decays with a time constant of about 50 ms (Kusick et al., 2022). In contrast, the contribution to PPF by the regular refilling process at lower frequencies, represented by the Ca^{2+}-dependent priming rate constant k_2 in the model,
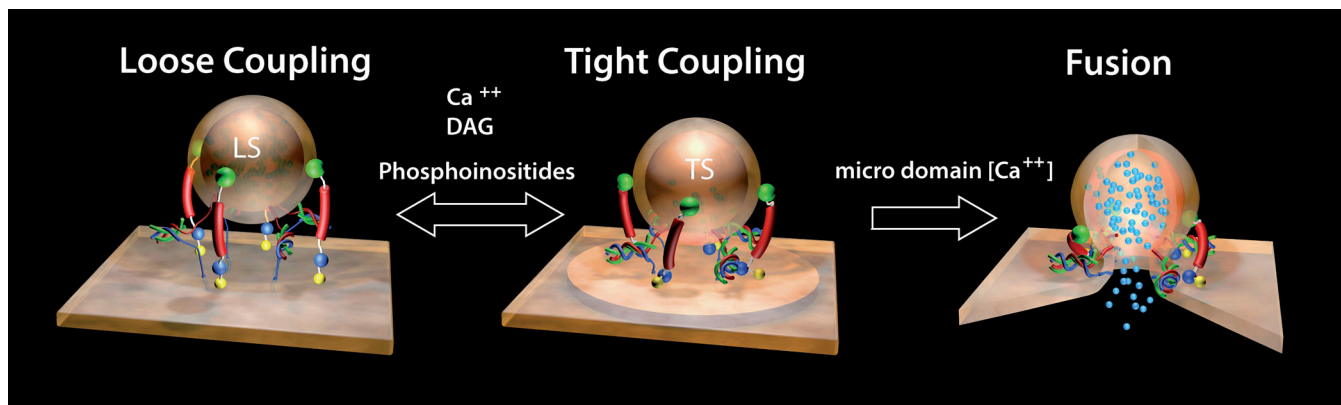
Heterogeneity in synaptic strength
May be caused by differences in the sizes of subpools LS and TS at rest
Redistribution of Synaptic Efficacy
May happen by changes in abundance of vesicles in state TS relative to state LS
Frequency facilitation
May be observed, if an AP shifts more vesicles from LS to TS than are released
Depression at low frequencies
The opposite to frequency facilitation: More vesicle consumption than resupply

Figure 4.   **Summary of alternative interpretations offered by the LS/TS model.** In all cases listed a shift in the LS/TS ratio can explain observed changes and differences without having to postulate a change in p_{fusion}. Regulatory domains on Munc13 and other presynaptic proteins, sensing second messengers such as $[Ca^{2+}]$, DAG, and phosphoinositides, provide options for modulation of neurotransmitter release over many time scales. The shape of molecules in the illustration, intended to represent SNAREs and Munc13, is hypothetical. Any other components of the release machinery are omitted for clarity.

is minor, although this process is enhanced by ($[Ca^{2+}]$) (Lin et al., 2022).

Commonly, PPF is called and discussed as such only, if the net effect results in PPR >1. In order for the calyx model to achieve such net facilitation, the release probability of the second stimulus needs to be increased by about 20% (half of the 40% reduction by depletion). Ca^{2+} current facilitation and saturation of Ca^{2+} buffers may contribute to this effect, as shown by detailed studies of these mechanisms (Borst and Sakmann, 1998; Cuttle et al., 1998; Rozov et al., 2001; Müller et al., 2008; Lin et al., 2012; Eisner et al., 2023). The finding of only a limited contribution of increased release probability to PPF is in line with a recent study at cerebellar synapses in which short-term plasticity at 100 Hz could fully be explained by a two-step priming model without the assumption of an increase in p_{fusion} (Miki et al., 2016). Common to both models of release at the cerebellar and calyx of Held synapse is the assumption that a large part of PPF is mediated by a change in occupancy of the fusion-competent vesicle state—in contrast to the dominating view that PPF mainly reflects p_{fusion}.

Taken together, the sequential two-step priming scheme provides options for the explanation of seemingly very different phenomena, such as short-term depression, frequency facilitation, and frequency invariance based on properties of the vesicle priming process, without having to postulate changes in the release probability of fully primed vesicles (Fig. 4). This does not exclude, however, that such changes may be responsible for certain plasticity features or else contribute to their fine-tuning.

Discussion

Conceiving the priming of synaptic vesicles as a reversible, dynamic, and regulated multistep process opens up novel options for the interpretation of the role of presynaptic proteins in short-term plasticity and in generating diversity of synaptic strength among synapses. In particular, many changes in synaptic function induced by molecular perturbations or pharmacological manipulations of synaptic proteins that previously were interpreted as changes in release probability can be understood—at least in part—as changes in the balance between fully primed (TS) vesicles and immaturely primed (LS) vesicles. This balance, in turn, is determined, next to release, by activity-dependent enhancement of priming. Several features of synapse heterogeneity and short-term plasticity can be explained on this basis, without postulating differences or changes in release probability. Unfortunately, distinguishing between this "priming-centered" view and alternative classical models by electrophysiological experiments alone is difficult, involving detailed statistical analysis of responses to stimulation trains (Miki et al., 2016; Lin et al., 2022) or consideration of specific properties of certain types of synapses (see above). In line with the arguments about the importance of priming, as discussed here, a recent study, using novel methods of fluctuation analysis, concluded that short-term depression at the hippocampal mossy fiber–CA3 interneuron synapse is the result of a reduction in site occupancy rather than in the probability of exocytosis (Tanaka et al., 2021). Thus, a deeper understanding of the processes leading to and controlling neurotransmitter release will certainly benefit from a combination

of molecular, optical, and functional studies (Blanchard et al., 2020). It is expected that this understanding will uncover the roles of several proteins in vesicle priming, which so far have been associated with the process of vesicle fusion.

Acknowledgments

References

Aldahabi, M., F. Balint, N. Holderith, A. Lorincz, M. Reva, and Z. Nusser. 2022. Different priming states of synaptic vesicles underlie distinct release probabilities at hippocampal excitatory synapses. Neuron. 110: 4144–4161.e7. https://doi.org/10.1016/j.neuron.2022.09.035

Atluri, P.P., and W.G. Regehr. 1996. Determinants of the time course of facilitation at the granule cell to Purkinje cell synapse. J. Neurosci. 16: 5661–5671. https://doi.org/10.1523/JNEUROSCI.16-18-05661.1996

Bagnall, M.W., L.E. McElvain, M. Faulstich, and S. du Lac. 2008. Frequency-independent synaptic transmission supports a linear vestibular behavior. Neuron. 60:343–352. https://doi.org/10.1016/j.neuron.2008.10.002

Betz, A., U. Ashery, M. Rickmann, I. Augustin, E. Neher, T.C. Südhof, J. Rettig, and N. Brose. 1998. Munc13-1 is a presynaptic phorbol ester receptor that enhances neurotransmitter release. Neuron. 21:123–136. https://doi.org/10.1016/S0896-6273(00)80520-6

Betz, W.J. 1970. Depression of transmitter release at the neuromuscular junction of the frog. J. Physiol. 206:629–644. https://doi.org/10.1113/jphysiol.1970.sp009034

Blanchard, K., J. Zorrilla de San Martín, A. Marty, I. Llano, and F.F. Trigo. 2020. Differentially poised vesicles underlie fast and slow components of release at single synapses. J. Gen. Physiol. 152:e201912523. https://doi.org/10.1085/jgp.201912523

Bornschein, G., S. Brachtendorf, and H. Schmidt. 2020. Developmental increase of neocortical presynaptic efficacy via maturation of vesicle replenishment. Front. Synaptic Neurosci. 11:36. https://doi.org/10.3389/fnsyn.2019.00036

Borst, J.G., and B. Sakmann. 1998. Facilitation of presynaptic calcium currents in the rat brainstem. J. Physiol. 513:149–155. https://doi.org/10.1111/j.1469-7793.1998.149by.x

Chamberland, S., A. Evstratova, and K. Tóth. 2014. Interplay between synchronization of multivesicular release and recruitment of additional release sites support short-term facilitation at hippocampal mossy fiber to CA3 pyramidal cells synapses. J. Neurosci. 34:11032–11047. https://doi.org/10.1523/JNEUROSCI.0847-14.2014

Chang, S., T. Trimbuch, and C. Rosenmund. 2018. Synaptotagmin-1 drives synchronous Ca^{2+}-triggered fusion by C_2B-domain-mediated synaptic-vesicle-membrane attachment. Nat. Neurosci. 21:33–40. https://doi.org/10.1038/s41593-017-0037-5

Chen, C., R. Satterfield, S.M. Young Jr., and P. Jonas. 2017. Triple function of synaptotagmin 7 ensures efficiency of high-frequency transmission at central GABAergic synapses. Cell Rep. 21:2082–2089. https://doi.org/10.1016/j.celrep.2017.10.122

Cuttle, M.F., T. Tsujimoto, I.D. Forsythe, and T. Takahashi. 1998. Facilitation of the presynaptic calcium current at an auditory synapse in rat brainstem. J. Physiol. 512:723–729. https://doi.org/10.1111/j.1469-7793.1998.723bd.x

Debanne, D., N.C. Guérineau, B.H. Gähwiler, and S.M. Thompson. 1996. Paired-pulse facilitation and depression at unitary synapses in rat hippocampus: Quantal fluctuation affects subsequent release. J. Physiol. 491:163–176. https://doi.org/10.1113/jphysiol.1996.sp021204

Del Castillo, J., and B. Katz. 1954. Quantal components of the end-plate potential. J. Physiol. 124:560–573. https://doi.org/10.1113/jphysiol.1954.sp005129

Delvendahl, I., A. Weyhersmüller, A. Ritzau-Jost, and S. Hallermann. 2013. Hippocampal and cerebellar mossy fibre boutons - same name, different function. J. Physiol. 591:3179–3188. https://doi.org/10.1113/jphysiol.2012.248294

Dittman, J.S. 2019. Unc13: A multifunctional synaptic marvel. Curr. Opin. Neurobiol. 57:17–25. https://doi.org/10.1016/j.conb.2018.12.011

Dittman, J.S., A.C. Kreitzer, and W.G. Regehr. 2000. Interplay between facilitation, depression, and residual calcium at three presynaptic terminals. J. Neurosci. 20:1374–1385. https://doi.org/10.1523/JNEUROSCI.20-04-01374.2000

Dittman, J.S., and W.G. Regehr. 1996. Contributions of calcium-dependent and calcium-independent mechanisms to presynaptic inhibition at a cerebellar synapse. J. Neurosci. 16:1623–1633. https://doi.org/10.1523/JNEUROSCI.16-05-01623.1996

Dittman, J.S., and W.G. Regehr. 1998. Calcium dependence and recovery kinetics of presynaptic depression at the climbing fiber to Purkinje cell synapse. J. Neurosci. 18:6147–6162. https://doi.org/10.1523/JNEUROSCI.18-16-06147.1998

Dobrunz, L.E., and C.F. Stevens. 1997. Heterogeneity of release probability, facilitation, and depletion at central synapses. Neuron. 18:995–1008. https://doi.org/10.1016/S0896-6273(00)80338-4

Doussau, F., H. Schmidt, K. Dorgans, A.M. Valera, B. Poulain, and P. Isope. 2017. Frequency-dependent mobilization of heterogeneous pools of synaptic vesicles shapes presynaptic plasticity. Elife. 6:e28935. https://doi.org/10.7554/eLife.28935

Eisner, D., E. Neher, H. Taschenberger, and G. Smith. 2023. Physiology of intracellular calcium buffering. Physiol. Rev. 103:2767–2845. https://doi.org/10.1152/physrev.00042.2022

Elmqvist, D., and D.M. Quastel. 1965. A quantitative study of end-plate potentials in isolated human muscle. J. Physiol. 178:505–529. https://doi.org/10.1113/jphysiol.1965.sp007639

Grande, G., and L.Y. Wang. 2011. Morphological and functional continuum underlying heterogeneity in the spiking fidelity at the calyx of Held synapse in vitro. J. Neurosci. 31:13386–13399. https://doi.org/10.1523/JNEUROSCI.0400-11.2011

Gustafsson, B., R. Ma, and E. Hanse. 2019. The small and dynamic pre-primed pool at the release site; A useful concept to understand release probability and short-term synaptic plasticity? Front. Synaptic Neurosci. 11:7. https://doi.org/10.3389/fnsyn.2019.00007

Hallermann, S., A. Fejtova, H. Schmidt, A. Weyhersmüller, R.A. Silver, E.D. Gundelfinger, and J. Eilers. 2010. Bassoon speeds vesicle reloading at a central excitatory synapse. Neuron. 68:710–723. https://doi.org/10.1016/j.neuron.2010.10.026

Hallermann, S., and R.A. Silver. 2013. Sustaining rapid vesicular release at active zones: Potential roles for vesicle tethering. Trends Neurosci. 36: 185–194. https://doi.org/10.1016/j.tins.2012.10.001

Harris, K.M., and J.K. Stevens. 1989. Dendritic spines of CA 1 pyramidal cells in the rat hippocampus: Serial electron microscopy with reference to their biophysical characteristics. J. Neurosci. 9:2982–2997. https://doi.org/10.1523/JNEUROSCI.09-08-02982.1989

He, E., K. Wierda, R. van Westen, J.H. Broeke, R.F. Toonen, L.N. Cornelisse, and M. Verhage. 2017. Munc13-1 and Munc18-1 together prevent NSF-dependent de-priming of synaptic vesicles. Nat. Commun. 8:15915. https://doi.org/10.1038/ncomms15915

Holderith, N., M. Aldahabi, and Z. Nusser. 2022. Selective enrichment of munc13-2 in presynaptic active zones of hippocampal pyramidal cells that innervate mGluR1 alpha expressing interneurons. Front Synaptic Neuro. 13:773209. https://doi.org/10.3389/fnsyn.2021.773209

Hosoi, N., T. Sakaba, and E. Neher. 2007. Quantitative analysis of calcium-dependent vesicle recruitment and its functional role at the calyx of Held synapse. J. Neurosci. 27:14286–14298. https://doi.org/10.1523/JNEUROSCI.4122-07.2007

Imig, C., S.W. Min, S. Krinner, M. Arancillo, C. Rosenmund, T.C. Südhof, J. Rhee, N. Brose, and B.H. Cooper. 2014. The morphological and molecular nature of synaptic vesicle priming at presynaptic active zones. Neuron. 84:416–431. https://doi.org/10.1016/j.neuron.2014.10.009

Jackman, S.L., J. Turecek, J.E. Belinsky, and W.G. Regehr. 2016. The calcium sensor synaptotagmin 7 is required for synaptic facilitation. Nature. 529: 88–91. https://doi.org/10.1038/nature16507

Jockusch, W.J., D. Speidel, A. Sigler, J.B. Sørensen, F. Varoqueaux, J.S. Rhee, and N. Brose. 2007. CAPS-1 and CAPS-2 are essential synaptic vesicle priming proteins. Cell. 131:796–808. https://doi.org/10.1016/j.cell.2007.11.002

Junge, H.J., J.S. Rhee, O. Jahn, F. Varoqueaux, J. Spiess, M.N. Waxham, C. Rosenmund, and N. Brose. 2004. Calmodulin and Munc13 form a Ca2+

sensor/effector complex that controls short-term synaptic plasticity. *Cell.* 118:389–401. https://doi.org/10.1016/j.cell.2004.06.029

Katz, B., and R. Miledi. 1968. The role of calcium in neuromuscular facilitation. *J. Physiol.* 195:481–492. https://doi.org/10.1113/jphysiol.1968.sp008469

Kobbersmed, J.R., A.T. Grasskamp, M. Jusyte, M.A. Böhme, S. Ditlevsen, J.B. Sørensen, and A.M. Walter. 2020. Rapid regulation of vesicle priming explains synaptic facilitation despite heterogeneous vesicle:Ca^{2+} channel distances. *Elife.* 9:e51032. https://doi.org/10.7554/eLife.51032

Kruse, M., O. Vivas, A. Traynor-Kaplan, and B. Hille. 2016. Dynamics of phosphoinositide-dependent signaling in sympathetic neurons. *J. Neurosci.* 36:1386–1400. https://doi.org/10.1523/JNEUROSCI.3535-15.2016

Kusick, G.F., T.H. Ogunmowo, and S. Watanabe. 2022. Transient docking of synaptic vesicles: Implications and mechanisms. *Curr. Opin. Neurobiol.* 74:102535. https://doi.org/10.1016/j.conb.2022.102535

Kusick, G.F., Z. Wu, M.M.M. Berns, S. Raychaudhuri, K. Itoh, A.M. Walter, E.R. Chapman, and S. Watanabe. 2023. Synaptotagmin 7 docks synaptic vesicles for Doc2α-triggered asynchronous neurotransmitter release. *Mol. Biol. Cell.* 34:212–213.

Lin, K.H., E. Erazo-Fischer, and H. Taschenberger. 2012. Similar intracellular Ca2+ requirements for inactivation and facilitation of voltage-gated Ca2+ channels in a glutamatergic mammalian nerve terminal. *J. Neurosci.* 32: 1261–1272. https://doi.org/10.1523/JNEUROSCI.3838-11.2012

Lin, K.H., H. Taschenberger, and E. Neher. 2022. A sequential two-step priming scheme reproduces diversity in synaptic strength and short-term plasticity. *Proc. Natl. Acad. Sci. USA.* 119:e2207987119. https://doi.org/10.1073/pnas.2207987119

Lipstein, N., S. Chang, K.H. Lin, F.J. López-Murcia, E. Neher, H. Taschenberger, and N. Brose. 2021. Munc13-1 is a Ca^{2+}-phospholipid-dependent vesicle priming hub that shapes synaptic short-term plasticity and enables sustained neurotransmission. *Neuron.* 109:3980–4000.e7. https://doi.org/10.1016/j.neuron.2021.09.054

Lipstein, N., T. Sakaba, B.H. Cooper, K.H. Lin, N. Strenzke, U. Ashery, J.S. Rhee, H. Taschenberger, E. Neher, and N. Brose. 2013. Dynamic control of synaptic vesicle replenishment and short-term plasticity by Ca(2+)-calmodulin-Munc13-1 signaling. *Neuron.* 79:82–96. https://doi.org/10.1016/j.neuron.2013.05.011

Liu, G., and R.W. Tsien. 1995. Properties of synaptic transmission at single hippocampal synaptic boutons. *Nature.* 375:404–408. https://doi.org/10.1038/375404a0

Liu, H., H. Bai, E. Hui, L. Yang, C.S. Evans, Z. Wang, S.E. Kwon, and E.R. Chapman. 2014. Synaptotagmin 7 functions as a Ca2+-sensor for synaptic vesicle replenishment. *Elife.* 3:e01524. https://doi.org/10.7554/eLife.01524

Lorteije, J.A., S.I. Rusu, C. Kushmerick, and J.G. Borst. 2009. Reliability and precision of the mouse calyx of Held synapse. *J. Neurosci.* 29: 13770–13784. https://doi.org/10.1523/JNEUROSCI.3285-09.2009

Losonczy, A., L. Zhang, R. Shigemoto, P. Somogyi, and Z. Nusser. 2002. Cell type dependence and variability in the short-term plasticity of EPSCs in identified mouse hippocampal interneurones. *J. Physiol.* 542:193–210. https://doi.org/10.1113/jphysiol.2002.020024

MacLeod, K.M., T.K. Horiuchi, and C.E. Carr. 2007. A role for short-term synaptic facilitation and depression in the processing of intensity information in the auditory brain stem. *J. Neurophysiol.* 97:2863–2874. https://doi.org/10.1152/jn.01030.2006

Mahfooz, K., M. Singh, R. Renden, and J.F. Wesseling. 2016. A well-defined readily releasable pool with fixed capacity for storing vesicles at calyx of Held. *PLoS Comput. Biol.* 12:e1004855. https://doi.org/10.1371/journal.pcbi.1004855

Malagon, G., T. Miki, V. Tran, L.C. Gomez, and A. Marty. 2020. Incomplete vesicular docking limits synaptic strength under high release probability conditions. *Elife.* 9:e52137. https://doi.org/10.7554/eLife.52137

Markram, H., and M. Tsodyks. 1996. Redistribution of synaptic efficacy between neocortical pyramidal neurons. *Nature.* 382:807–810. https://doi.org/10.1038/382807a0

Maus, L., C. Lee, B. Altas, S.M. Sertel, K. Weyand, S.O. Rizzoli, J. Rhee, N. Brose, C. Imig, and B.H. Cooper. 2020. Ultrastructural correlates of presynaptic functional heterogeneity in hippocampal synapses. *Cell Rep.* 30:3632–3643.e8. https://doi.org/10.1016/j.celrep.2020.02.083

Meyer, A.C., E. Neher, and R. Schneggenburger. 2001. Estimation of quantal size and number of functional active zones at the calyx of Held synapse by nonstationary EPSC variance analysis. *J. Neurosci.* 21:7889–7900. https://doi.org/10.1523/JNEUROSCI.21-20-07889.2001

Midorikawa, M., and T. Sakaba. 2017. Kinetics of releasable synaptic vesicles and their plastic changes at hippocampal mossy fiber synapses. *Neuron.* 96:1033–1040.e3. https://doi.org/10.1016/j.neuron.2017.10.016

Miki, T., G. Malagon, C. Pulido, I. Llano, E. Neher, and A. Marty. 2016. Actin- and myosin-dependent vesicle loading of presynaptic docking sites prior to exocytosis. *Neuron.* 91:808–823. https://doi.org/10.1016/j.neuron.2016.07.033

Miki, T., Y. Nakamura, G. Malagon, E. Neher, and A. Marty. 2018. Two-component latency distributions indicate two-step vesicular release at simple glutamatergic synapses. *Nat. Commun.* 9:3943. https://doi.org/10.1038/s41467-018-06336-5

Müller, M., F. Felmy, and R. Schneggenburger. 2008. A limited contribution of Ca2+ current facilitation to paired-pulse facilitation of transmitter release at the rat calyx of Held. *J. Physiol.* 586:5503–5520. https://doi.org/10.1113/jphysiol.2008.155838

Murthy, V.N., and C.F. Stevens. 1999. Reversal of synaptic vesicle docking at central synapses. *Nat. Neurosci.* 2:503–507. https://doi.org/10.1038/9149

Neher, E. 2015. Merits and limitations of vesicle pool models in view of heterogeneous populations of synaptic vesicles. *Neuron.* 87:1131–1142. https://doi.org/10.1016/j.neuron.2015.08.038

Neher, E., and N. Brose. 2018. Dynamically primed synaptic vesicle states: Key to understand synaptic short-term plasticity. *Neuron.* 100: 1283–1291. https://doi.org/10.1016/j.neuron.2018.11.024

Neher, E., and H. Taschenberger. 2021. Non-negative matrix factorization as a tool to distinguish between synaptic vesicles in different functional states. *Neuroscience.* 458:182–202. https://doi.org/10.1016/j.neuroscience.2020.10.012

Nicoll, R.A., and D. Schmitz. 2005. Synaptic plasticity at hippocampal mossy fibre synapses. *Nat. Rev. Neurosci.* 6:863–876. https://doi.org/10.1038/nrn1786

Pan, B., and R.S. Zucker. 2009. A general model of synaptic transmission and short-term plasticity. *Neuron.* 62:539–554. https://doi.org/10.1016/j.neuron.2009.03.025

Prinslow, E.A., K.P. Stepien, Y.Z. Pan, J. Xu, and J. Rizo. 2019. Multiple factors maintain assembled trans-SNARE complexes in the presence of NSF and αSNAP. *Elife.* 8:e38880. https://doi.org/10.7554/eLife.38880

Pulido, C., and A. Marty. 2018. A two-step docking site model predicting different short-term synaptic plasticity patterns. *J. Gen. Physiol.* 150: 1107–1124. https://doi.org/10.1085/jgp.201812072

Quastel, D.M. 1997. The binomial model in fluctuation analysis of quantal neurotransmitter release. *Biophys. J.* 72:728–753. https://doi.org/10.1016/S0006-3495(97)78709-5

Rhee, J.S., A. Betz, S. Pyott, K. Reim, F. Varoqueaux, I. Augustin, D. Hesse, T.C. Südhof, M. Takahashi, C. Rosenmund, and N. Brose. 2002. Beta phorbol ester- and diacylglycerol-induced augmentation of transmitter release is mediated by Munc13s and not by PKCs. *Cell.* 108:121–133. https://doi.org/10.1016/S0092-8674(01)00635-3

Ritzau-Jost, A., L. Jablonski, J. Viotti, N. Lipstein, J. Eilers, and S. Hallermann. 2018. Apparent calcium dependence of vesicle recruitment. *J. Physiol.* 596:4693–4707. https://doi.org/10.1113/JP275911

Rizo, J. 2022. Molecular mechanisms underlying neurotransmitter release. *Annu. Rev. Biophys.* 51:377–408. https://doi.org/10.1146/annurev-biophys-111821-104732

Rosenmund, C., A. Sigler, I. Augustin, K. Reim, N. Brose, and J.S. Rhee. 2002. Differential control of vesicle priming and short-term plasticity by Munc13 isoforms. *Neuron.* 33:411–424. https://doi.org/10.1016/S0896-6273(02)00568-8

Rosenmund, C., and C.F. Stevens. 1996. Definition of the readily releasable pool of vesicles at hippocampal synapses. *Neuron.* 16:1197–1207. https://doi.org/10.1016/S0896-6273(00)80146-4

Rozov, A., N. Burnashev, B. Sakmann, and E. Neher. 2001. Transmitter release modulation by intracellular Ca2+ buffers in facilitating and depressing nerve terminals of pyramidal cells in layer 2/3 of the rat neocortex indicates a target cell-specific difference in presynaptic calcium dynamics. *J. Physiol.* 531:807–826. https://doi.org/10.1111/j.1469-7793.2001.0807h.x

Scheuss, V., and E. Neher. 2001. Estimating synaptic parameters from mean, variance, and covariance in trains of synaptic responses. *Biophys. J.* 81: 1970–1989. https://doi.org/10.1016/S0006-3495(01)75848-1

Schlüter, O.M., F. Schmitz, R. Jahn, C. Rosenmund, and T.C. Südhof. 2004. A complete genetic analysis of neuronal Rab3 function. *J. Neurosci.* 24: 6629–6637. https://doi.org/10.1523/JNEUROSCI.1610-04.2004

Schuhmacher, M., A.T. Grasskamp, P. Barahtjan, N. Wagner, B. Lombardot, J.S. Schuhmacher, P. Sala, A. Lohmann, I. Henry, A. Shevchenko, et al. 2020. Live-cell lipid biochemistry reveals a role of diacylglycerol side-chain composition for cellular lipid dynamics and protein affinities. *Proc. Natl. Acad. Sci. USA.* 117:7729–7738. https://doi.org/10.1073/pnas.1912684117

Shin, O.H., J. Lu, J.S. Rhee, D.R. Tomchick, Z.P. Pang, S.M. Wojcik, M. Ca-macho-Perez, N. Brose, M. Machius, J. Rizo, et al. 2010. Munc13 C2B domain is an activity-dependent Ca2+ regulator of synaptic exocytosis. *Nat. Struct. Mol. Biol.* 17:280–288. https://doi.org/10.1038/nsmb.1758

Silva, M., V. Tran, and A. Marty. 2021. Calcium-dependent docking of synaptic vesicles. *Trends Neurosci.* 44:579–592. https://doi.org/10.1016/j.tins.2021.04.003

Silver, R.A. 2003. Estimation of nonuniform quantal parameters with multiple-probability fluctuation analysis: Theory, application and limitations. *J. Neurosci. Methods.* 130:127–141. https://doi.org/10.1016/j.jneumeth.2003.09.030

Smith, C., T. Moser, T. Xu, and E. Neher. 1998. Cytosolic Ca2+ acts by two separate pathways to modulate the supply of release-competent vesicles in chromaffin cells. *Neuron.* 20:1243–1253. https://doi.org/10.1016/S0896-6273(00)80504-8

Stevens, C.F., and J.F. Wesseling. 1998. Activity-dependent modulation of the rate at which synaptic vesicles become available to undergo exocytosis. *Neuron.* 21:415–424. https://doi.org/10.1016/S0896-6273(00)80550-4

Sun, H.Y., S.A. Lyons, and L.E. Dobrunz. 2005. Mechanisms of target-cell specific short-term plasticity at Schaffer collateral synapses onto interneurones versus pyramidal cells in juvenile rats. *J. Physiol.* 568:815–840. https://doi.org/10.1113/jphysiol.2005.093948

Tanaka, M., T. Sakaba, and T. Miki. 2021. Quantal analysis estimates docking site occupancy determining short-term depression at hippocampal glutamatergic synapses. *J. Physiol.* 599:5301–5327. https://doi.org/10.1113/JP282235

Taschenberger, H., A. Woehler, and E. Neher. 2016. Superpriming of synaptic vesicles as a common basis for intersynapse variability and modulation of synaptic strength. *Proc. Natl. Acad. Sci. USA.* 113:E4548–E4557. https://doi.org/10.1073/pnas.1606383113

Tawfik, B., J.S. Martins, S. Houy, C. Imig, P.S. Pinheiro, S.M. Wojcik, N. Brose, B.H. Cooper, and J.B. Sørensen. 2021. Synaptotagmin-7 places dense-core vesicles at the cell membrane to promote Munc13-2- and Ca^{2+}-dependent priming. *Elife.* 10:e64527. https://doi.org/10.7554/eLife.64527

Tewson, P., M. Westenberg, Y. Zhao, R.E. Campbell, A.M. Quinn, and T.E. Hughes. 2012. Simultaneous detection of Ca2+ and diacylglycerol signaling in living cells. *PLoS One.* 7:e42791. https://doi.org/10.1371/journal.pone.0042791

Thanawala, M.S., and W.G. Regehr. 2016. Determining synaptic parameters using high-frequency activation. *J. Neurosci. Methods.* 264:136–152. https://doi.org/10.1016/j.jneumeth.2016.02.021

Toth, K., G. Suares, J.J. Lawrence, E. Philips-Tansey, and C.J. McBain. 2000. Differential mechanisms of transmission at three types of mossy fiber synapse. *J. Neurosci.* 20:8279–8289. https://doi.org/10.1523/JNEUROSCI.20-22-08279.2000

Turecek, J., S.L. Jackman, and W.G. Regehr. 2016. Synaptic specializations support frequency-independent Purkinje cell output from the cerebellar cortex. *Cell Rep.* 17:3256–3268. https://doi.org/10.1016/j.celrep.2016.11.081

Turecek, J., S.L. Jackman, and W.G. Regehr. 2017. Synaptotagmin 7 confers frequency invariance onto specialized depressing synapses. *Nature.* 551:503–506. https://doi.org/10.1038/nature24474

Turecek, J., and W.G. Regehr. 2018. Synaptotagmin 7 mediates both facilitation and asynchronous release at granule cell synapses. *J. Neurosci.* 38:3240–3251. https://doi.org/10.1523/JNEUROSCI.3207-17.2018

Varela, J.A., K. Sen, J. Gibson, J. Fost, L.F. Abbott, and S.B. Nelson. 1997. A quantitative description of short-term plasticity at excitatory synapses in layer 2/3 of rat primary visual cortex. *J. Neurosci.* 17:7926–7940. https://doi.org/10.1523/JNEUROSCI.17-20-07926.1997

Vere-Jones, D. 1966. Simple stochastic models for the release of quanta of transmitter from a nerve terminal. *Aust. J. Stat.* 8:53–63. https://doi.org/10.1111/j.1467-842X.1966.tb00164.x

Wang, L.Y., and L.K. Kaczmarek. 1998. High-frequency firing helps replenish the readily releasable pool of synaptic vesicles. *Nature.* 394:384–388. https://doi.org/10.1038/28645

Watanabe, S. 2016. Flash-and-Freeze: Coordinating optogenetic stimulation with rapid freezing to visualize membrane dynamics at synapses with millisecond resolution. *Front. Synaptic Neurosci.* 8:24. https://doi.org/10.3389/fnsyn.2016.00024

Weichard, I., H. Taschenberger, F. Gsell, G. Bornschein, A. Ritzau-Jost, H. Schmidt, R.J. Kittel, J. Eilers, E. Neher, S. Hallermann, and J. Nerlich. 2023. Fully-primed slowly-recovering vesicles mediate presynaptic LTP at neocortical neurons. *Proc. Natl. Acad. Sci. USA.* 120:e2305460120. https://doi.org/10.1073/pnas.2305460120

Weingarten, D.J., A. Shrestha, K. Juda-Nelson, S.A. Kissiwaa, E. Spruston, and S.L. Jackman. 2022. Fast resupply of synaptic vesicles requires synaptotagmin-3. *Nature.* 611:320–325. https://doi.org/10.1038/s41586-022-05337-1

Worden, M.K., M. Bykhovskaia, and J.T. Hackett. 1997. Facilitation at the lobster neuromuscular junction: A stimulus-dependent mobilization model. *J. Neurophysiol.* 78:417–428. https://doi.org/10.1152/jn.1997.78.1.417

Zucker, R.S., and W.G. Regehr. 2002. Short-term synaptic plasticity. *Annu. Rev. Physiol.* 64:355–405. https://doi.org/10.1146/annurev.physiol.64.092501.114547